Available online at www.sciencedirect.com
ScienceDirect
European Polymer Journal 43 (2007) 2708–2717
EUROPEAN POLYMER JOURNAL
www.elsevier.com/locate/europolj

Electrical impedance spectroscopy of epoxy systems II: Molar fraction variation, resistivity, capacitance and relaxation processes of 1,4-butanediol diglycidyl ether/succinic anhydride and triethylamine as initiator

Aline Nicolau [a], Ana M. Nucci [a], Emilse M.A. Martini [b], Dimitrios Samios [a,*]

[a] *Laboratório de Instrumentação e Dinâmica Molecular, Instituto de Química, Universidade Federal do Rio Grande do Sul, Av. Bento Gonçalves 9500, Caixa Postal 15003, CEP 91501-970, Porto Alegre, Brazil*

[b] *Laboratório de Eletroquímica, Instituto de Química Universidade Federal do Rio Grande do Sul, Av. Bento Gonçalves 9500, Caixa Postal 15003, CEP 91501-970, Porto Alegre, Brazil*

Received 30 May 2006; received in revised form 28 December 2006; accepted 12 March 2007
Available online 16 March 2007

Abstract

The Electric Impedance Spectroscopy (EIS) was used to evaluate resistivity, capacitance and relaxation processes of a cured epoxy system with different molar composition of 1,4-butanediol diglycidyl ether (EP), succinic anhydride (SA) and triethylamine (TEA) as initiator. The measurements were done over range frequencies between 10^{-1} and 10^{5} Hz. The systematic change of the molar fraction composition affected the resistivity and capacitance changes indicating gelation critical compositions according to the Flory's aggregation theory. The complex electric functions, dielectric constant $\varepsilon^{\bullet}$, electric modulus $M^{\bullet}$, impedance $Z^{\bullet}$, admittance $Y^{\bullet}$ and the loss factor tan δ were utilized in order to investigate the relaxation processes. Relaxation peaks were observed for different molar fraction composition only in the imaginary impedance, the electric modulus and the tan δ as frequency functions. The relaxation frequencies obtained by Z'', M'' and tan δ evaluation are distinct and have been discussed in terms of resin components molar fraction dependence.

Keywords: Electrical impedance spectroscopy; Epoxy systems; Molar fraction variation; Relaxation processes

1. Introduction

The epoxy resins are widely used due to the capability of the epoxide ring to react with a variety of substrates. The reaction with curing agents gives insoluble and intractable thermoset polymers. High chemical and corrosion resistance, good mechanical, thermal and electrical properties, adhesion to various substrates are characteristics of these resins. Because their versatility, the epoxy resins are used in thousands of industrial applications. In the electronic industry, for example, they are utilized as insulators, protective coatings, adhesives of high resistance, among other applications [1,2]. Depending on the

* Corresponding author.
E-mail address: dsamios@iq.ufrgs.br (D. Samios).

0014-3057/$ - see front matter © 2007 Elsevier Ltd. All rights reserved.
doi:10.1016/j.eurpolymj.2007.03.018

temperature, time, and formulation of the cure reaction for a same system, it is possible to obtain different mechanical and electrical properties of the macromolecular structure at the end of the polymerization. The determination of the electric properties of these dielectric materials and their variation with frequency provide valuable information that allows to study the molecular dynamic, the relaxation processes and their correct utilization for a specific electronic application.

The dielectric measurements have been a subject of interest to various research groups [3–24]. Part of these publications aims the evolution of the dielectric properties of fixed composition polymeric systems during cure reaction. In our earlier studies with epoxy systems [25–28] we focused on the composition varying the molar ratio of mixtures between epoxy and anhydride. This methodology permitted to establish knowledge about the kinetic of the curing process and the physical properties of the final products. In this work the Electric Impedance Spectroscopy (EIS) was used to investigate the resistivity and capacitance changes through the variation of the molar fraction of the epoxy system and evaluate the characteristics of the relaxation processes present in the samples after cure reaction. The evaluation of the complex electric functions (dielectric constant $\varepsilon^{\bullet}$, electric modulus $M^{\bullet}$, impedance $Z^{\bullet}$, admittance $Y^{\bullet}$ and the loss factor $\tan\delta$) as functions of frequency permits to detect the presence of relaxation processes in the studied epoxy system and relating them to the molar fraction composition of the system. The study was done over a wide range of epoxy composition, including mixtures with anhydride excess, stoichiometric formulation and epoxy excess. It is expected that the variation of the composition affects the dynamic and consequently the dielectric properties of the material [29]. The gelation characteristics of molecular systems with polyfunctionality were predicted by Flory and constitute one of the important aspects of the evaluation of the curing processes. In this way, the aim of this paper is, by using the Electric Impedance Spectroscopy technique, to extend the knowledge about dielectric properties and relaxation processes of cured epoxy systems over a wide composition range which allows to elucidate the role of the molar composition in relation to them. It is well known [28,30,31] that the solidification during the curing process starts with initial elevation of the viscosity of the reaction mixture followed by gelation and finally the vitrification of the sample. The reactants of the epoxy and the anhydride used in this study are polyfunctional materials and the produced samples, with different compositions, correspond to different degrees of aggregation reflecting the physical state namely: the state before gelation, the state with gelation and finally the vitreous state of the system. Therefore, this study aims to evaluate the relation between the dielectric properties, the relaxation processes and the physical state of the studied epoxy system in relation to the composition.

2. Background

When an electric field is applied to a capacitor plates separated by a dielectric material like an epoxy resin or other polymeric specimen, the electric charges of atoms, molecules and ions suffer local displacement relative to their original equilibrium positions and the material is polarized. Generally the polarization can be classified in four categories namely: electronic, atomic, dipolar and migrating charges polarization [3,7]. The dielectric relaxation processes are normally related to one or more polarization processes of the studied material. Generally, every relaxation process is characterized by a relaxation time specific of the process. The contributions of atomic and electronic charges, which occur at still higher frequencies, are considered to be instantaneous in dielectric studies of polymers. Therefore, the two major components of the dielectric response of polymers in an applied electric field are the dipolar polarization and the polarization due migrating charges. Dipolar and migrating charge polarizations can be detected in frequencies smaller than 10^9 Hz. This reality requires a very wide frequency range of ac potential in order to detect all kind of polarization. Specifically, the lower frequency range is dominated by the migration of the charges. The experiments of the present study were performed in the low frequency range, between 10^{-1} to 10^5 Hz.

The investigation of the different electric properties of a dielectric material permits to obtain the dynamic behavior in terms of relaxation processes. These properties are always presented as complex functions related to the complex dielectric constant ε^*, frequently denominated complex permittivity:

$$\varepsilon^* = \varepsilon' - j\varepsilon''. \tag{1}$$

Other complex electric functions are given by Eqs. (2)–(5). All of them are directly related to ε^*.

Complex electric modulus:

$$M^* = M' + jM'' = \frac{1}{\varepsilon^*}. \tag{2}$$

Complex electric impedance:

$$Z^* = Z' - jZ'' = \frac{1}{j\omega C_0 \varepsilon^*}. \tag{3}$$

Complex electric admittance:

$$Y^* = Y' + jY'' = j\omega C_0 \varepsilon^*. \tag{4}$$

Loss factor:

$$\tan\delta = \frac{\varepsilon''}{\varepsilon'} = \frac{M''}{M'} = \frac{Z'}{Z''} = \frac{Y'}{Y''}. \tag{5}$$

In these equations, $j = \sqrt{-1}$, $\omega = 2\pi f$ and C_0, the geometric capacitance of the cell, defined as:

$$C_0 = \frac{\varepsilon_0 S}{L} \tag{6}$$

where S is the area of capacitor plates and L is the distance between them.

The simplest model to describe a dielectric relaxation was deduced by Debye assuming one characteristic relaxation time for the system. The frequency depended complex dielectric constant is given by Eq. (7):

$$\varepsilon^* = \varepsilon_u + \frac{(\varepsilon_r - \varepsilon_u)}{(1 + j\omega\tau)}, \tag{7}$$

where ε_u is the unrelaxated dielectric constant, i.e. the baseline value of the dielectric permittivity non-inclusive of the contributions of dipole orientation and free charge migration. The relaxed dielectric constant ε_r corresponds to the highest degree of dipole orientation attainable in the sample under given conditions, ω is the angular frequency and τ the Debye relaxation time. Using the Eqs. (1) and (7) and separating the real and imaginary components, one obtains:

$$\varepsilon' = \varepsilon_u + \frac{(\varepsilon_r - \varepsilon_u)}{1 + (\omega^2\tau^2)} \tag{8}$$

$$\varepsilon'' = \frac{(\varepsilon_r - \varepsilon_u)\omega\tau}{1 + (\omega^2\tau^2)}. \tag{9}$$

For different relaxation processes, where the one relaxation time Debye model can not describe the relaxation behavior, a model is introduced based on a relaxation time distribution as given by Eq. (10):

$$\varepsilon^* = \varepsilon_u + \frac{\varepsilon_r - \varepsilon_u}{1 + (j\chi)^{1-\alpha}}, \tag{10}$$

where α is the distribution parameter and $\chi = \omega\tau$. When $\alpha = 0$, Eq. (10) is the same as Eq. (7). Separating the real and imaginary components, one obtains [32]:

$$\varepsilon' = \varepsilon_u + \frac{(\varepsilon_r - \varepsilon_u)\left(1 + \chi^{1-\alpha}\sin\frac{\pi}{2}\alpha\right)}{1 + 2\chi^{1-\alpha}\sin\frac{\pi}{2}\alpha + \chi^{2(1-\alpha)}}, \tag{11}$$

$$\varepsilon'' = \frac{(\varepsilon_r - \varepsilon_u)\chi^{1-\alpha}\cos\frac{\pi}{2}\alpha}{1 + 2\chi^{1-\alpha}\sin\frac{\pi}{2}\alpha + \chi^{2(1-\alpha)}}. \tag{12}$$

As mentioned earlier, the dielectric response of polymeric materials generally comprises two phenomena, dipole orientation and charge migration. To account for conductivity due migrating charges, the Eq. (12) can be written in the form [32]:

$$\varepsilon'' = \frac{(\varepsilon_r - \varepsilon_u)\chi^{1-\alpha}\cos\frac{\pi}{2}\alpha}{1 + 2\chi^{1-\alpha}\sin\frac{\pi}{2}\alpha + \chi^{2(1-\alpha)}} + \frac{\sigma}{\omega\varepsilon_0}, \tag{13}$$

where σ is the conductivity related to the charge migration and ε_0 the vacuum dielectric constant. Gerhardt [32,33] demonstrated that the presence of a relaxation in the frequency depended representation of an electric property is strongly related to the ratio $r = \varepsilon_r/\varepsilon_u$. The evaluation and the comparison of the frequency graphics of the imaginary parts of the electric functions becomes extremely useful to determine the presence and to characterize the respective relaxation processes.

3. Experimental section

3.1. Materials

The samples studied in this work are the products after curing of a series of mixtures of 1,4-butanediol diglycidyl ether (EP) with succinic anhydride (SA) and triethylamine (TEA) as initiator, all of them provided by Aldrich Chemical Co. with analytical grade. Fig. 1 shows the chemical structures of the reactants. Table 1 summarizes the molar compositions of the mixtures before the curing in terms of x_{EP}, x_{SA} and x_{TEA} respectively, where x is the molar fraction of the components. The samples have a constant TEA molar fraction, $x_{TEA} = 0.0017$, that functions as an initiator for the reaction. As it can be seen in Table 1, the sample 7 corresponds to the stoichiometric composition and is a reference system. Additional to the stoichiometric sample, two other series with excess components were studied: one series with anhydride excess (samples 1–6), where the x_{EP} runs between 0.03 and 0.24, and

1,4-butanodiol diglycidyl ether

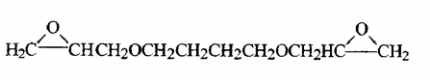

succinic anhydride

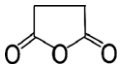

triethylamine

$N(CH_2CH_3)_3$

Fig. 1. The chemical structures of the reactants.

Table 1
Molar compositions of the mixtures before the curing in terms of x_{EP}

Anhydride excess samples							
Sample number	1	2	3	4	5	6	
x_{EP}	0.03	0.07	0.10	0.14	0.18	0.24	
Stoichiometric sample							
Sample number	7						
x_{EP}	0.31						
Epoxy excess samples							
Sample number	8	9	10	11	12	13	14
x_{EP}	0.36	0.48	0.57	0.67	0.76	0.86	1.00

another one (samples 8–14) with epoxy excess, x_{EP} from 0.36 to 1.00.

3.2. Sample preparation

All samples were prepared by mixing the three components with continuous stirring for about 15 min at room temperature (20 °C) according to Table 1. Immediately, after mixing, the mixture, adequately conditioned, was cured in pre-heated oven at 120 °C during 1 h. The obtained materials were stored in a desiccator at room temperature until the measurements were performed. All EIS measurements have been performed twenty four hours after curing.

3.3. Apparatus and procedures

Fig. 2 shows schematically the cell developed for the EIS measurements. The cell consists of a capacitor, constituted externally by stainless steel and internally by brass electrodes embedded in Teflon.

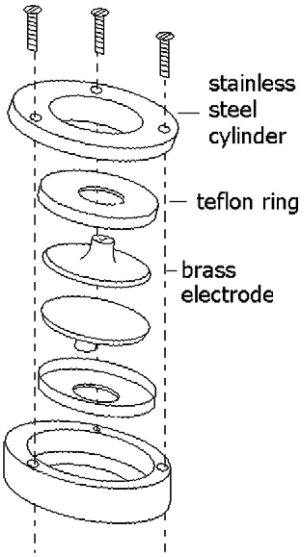

Fig. 2. The electric impedance cell.

The cured samples were placed between the electrodes, and by means of adequate cables, the cell was connected in to the Frequency Response Analyzer. The samples with very high epoxy (EP) or succinic anhydride (SA) excess do not present gelation, in this case the cured viscous sample was placed between the discs and they were separated by four small (2 mm × 2 mm) pieces of analytical grade filter paper.

The Electrical Impedance Spectroscopy experiments were carried out in a potentiostat with a frequency response analyzer, AUTOLAB PGSTAT 30/FRA2, in the frequency range between 10^{-1} and 10^5 Hz, controlled by a personal computer equipped with adequate software for data acquisition and treatment. A cc potential of 1 V and an ac signal with 5 mV amplitude was applied to the system. Ten experimental points have been recorded in every frequency decade. All experiments have been repeated three times in order to verify variation of the system during the measurements and to test repeatability. The cell constant K for every sample was obtained by using the relation $K = S/L$, where S is the electrode area and L the sample thickness.

4. Results and discussion

4.1. Electric properties evaluation

The complex permittivity (ε^*) data were obtained by using Eq. (3) and the experimentally obtained

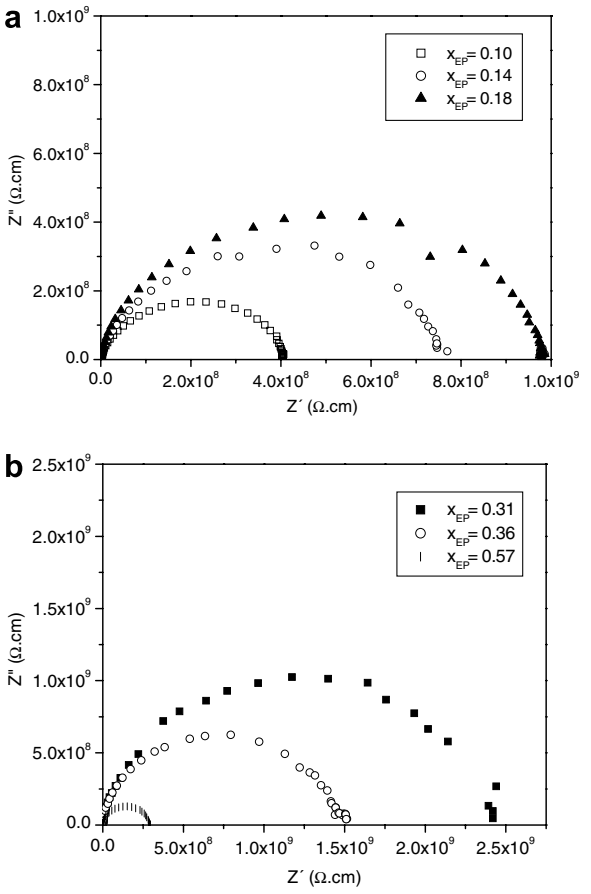

Fig. 3. Nyquist diagrams (Z' versus Z'') for anhydride and epoxy excesses (3a and 3b), respectively.

electric impedance values of the different samples. The ε' versus ε'' representation indicated extended and not complete semicircles due to high values of $r = \varepsilon_r/\varepsilon_u$, however, as it can be seen in Fig. 3, the impedance (Z' versus Z'') plots are characterized by well defined semicircles.

The experimental electrical impedance data were evaluated using a simple least square fit procedure and considering the equivalent circuit described in Fig. 4. The choice of this circuit was a compromise between a reasonable fitting of the experimental values and maintenance of the number of circuit elements at a minimum and still permitting the association of these elements to the phenomena probably occurring in the epoxy system.

The total impedance associated to the circuit before is given by Eq. (14).

$$Z_T = \frac{R_o + R_p + \omega^2 C^2 R_o R_p^2}{1 + \omega^2 C^2 R_p^2} - \frac{j\omega C R_p^2}{1 + \omega^2 C^2 R_p^2}, \qquad (14)$$

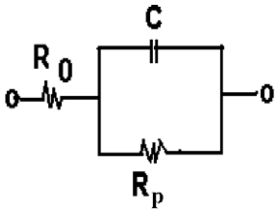

Fig. 4. Electric equivalent circuit.

where

$$Z' = \frac{R_o + R_p + \omega^2 C^2 R_o R_p^2}{1 + \omega^2 C^2 R_p^2}, \qquad (15)$$

$$Z'' = \frac{\omega C R_p^2}{1 + \omega^2 C^2 R_p^2}. \qquad (16)$$

R_o and R_p are the resistances in the upper and lower frequency limits respectively ($\omega \to \infty$ and $\omega \to 0$).

From Eq. (16) we obtain:

$$\frac{dZ''}{d\omega} = \frac{C R_p^2 (1 - \omega^2 R_p^2 C^2)}{1 + \omega^2 R_p^2 C^2}. \qquad (17)$$

This tends to zero when:

$$\omega = \frac{1}{R_p C}. \qquad (18)$$

Under this condition, using Eqs. (17) and (18), it results [3–5] to Eq. (19):

$$Z''_{max} = \frac{R_p}{2}. \qquad (19)$$

Fig. 3a and b shows part of the obtained Nyquist diagrams for samples with anhydride and epoxy excess respectively. For low frequency values the capacitor related impedance achieves very high values (Eq. (20)) and the circuit behaves as an open one.

$$Z_{capacitor} = \frac{1}{2\pi f C}. \qquad (20)$$

In this case the equivalent circuit in Fig. 4 is reduced in to the resistances $R_o + R_p$. In the high frequency range the capacitor associated impedance is practically zero and the equivalent circuit is reduced to R_o. In this way, the Nyquist diagram provides both values, namely R_o and $R_o + R_p$.

Fig. 5a and b shows the Bode diagrams ($\log|Z|$ versus $\log f$) for anhydride and epoxy excess respectively. In this representation, the value of $R_o + R_p$ is obtained in the low frequencies, from the

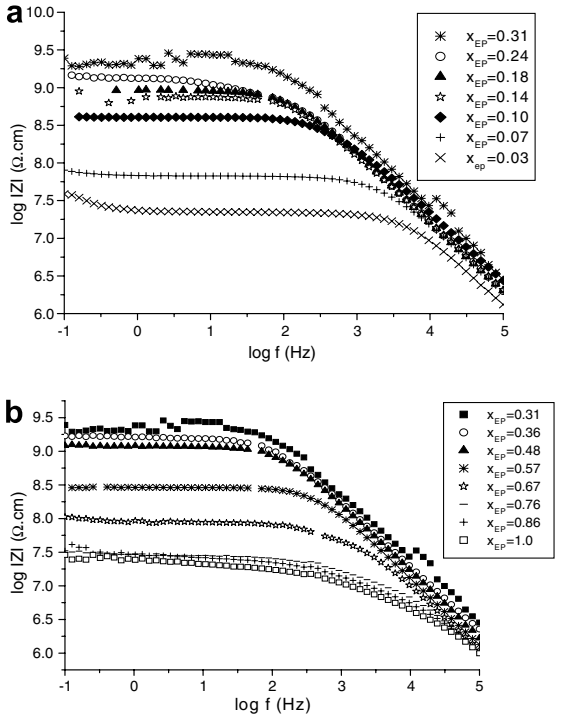

Fig. 5. Bode diagrams ($\log|Z|$ versus $\log f$) for anhydride and epoxy excesses (5a and 5b) respectively.

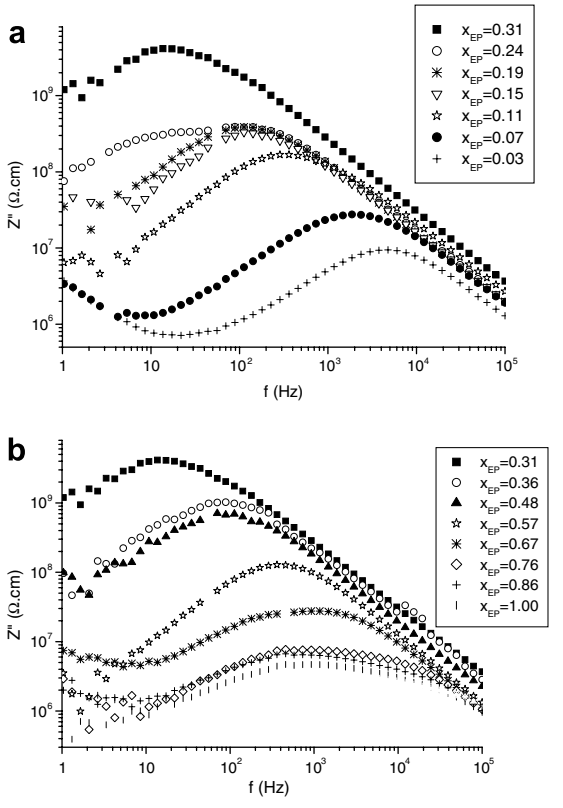

Fig. 6. $\log Z''$ versus $\log f$ diagrams for anhydride and epoxy excesses (6a and 6b) respectively.

intersection of the extrapolated frequency-independent horizontal line and the $\log|Z|$ axis.

Fig. 6a and b present diagrams of $\log Z''$ versus $\log f$ for samples with anhydride and epoxy excesses respectively. R_p is obtained by using Eq. (19).

The resistivity was evaluated by using Nyquist, Bode and $\log Z''$ versus $\log f$ diagrams. The Z-values of the diagrams were transformed by using the cell constant K which permitted to obtain directly the R_p and consequently the corresponding resistivity value (ρ). The relation between R_p, ρ and cell constant K (S and L electrode surface and spacing respectively) is:

$$\rho = R_p K = \frac{R_p S}{L}. \tag{21}$$

Table 2 resumes the resistivity values of the studied samples obtained according to the three different methods, described above. It is to observe that these values are very similar. The resistivity was determined in a frequency range where it is to expect that the polarization is attributed more to the migrating charges and less to the dipolar polarization. In the same table is included the capacitance data of samples with different molar compositions. The capacitance was obtained from the Eq. (20).

Table 2
Resistivity and capacitance values obtained according to Nyquist, Bode and $\log Z''$ versus $\log f$ diagrams

x_{EP}	$\rho_{Bode\times10^8}$ (Ω cm)	$\rho_{Z''\times10^8}$ (Ω cm)	$\rho_{Nyquist\times10^8}$ (Ω cm)	$C\times10^{-12}$ (F/cm)
0.03	0.23	0.19	0.22	7.80
0.07	0.68	0.55	0.67	3.64
0.10	4.1	3.4	4.1	2.11
0.14	7.6	6.6	7.5	2.70
0.18	9.5	7.7	9.3	2.19
0.24	13.2	7.8	13.8	2.30
0.31	21.4	20.5	24.3	1.29
0.36	16.4	14.1	15.9	1.26
0.48	11.9	10.1	12.1	1.15
0.57	2.9	2.8	2.9	2.33
0.67	0.89	0.55	0.91	4.09
0.76	0.31	0.15	0.29	18.7
0.86	0.29	0.13	0.28	48.0
1.00	0.24	0.09	0.23	33.0

4.2. Molar fraction variation/physical phase changing/resistivity and capacitance

This chapter presents an attempt to elucidate the effect of molar fraction variation on the samples

physical phase characteristics, using the resistivity and capacitance data, as resumed in Fig. 7a and b, and relating them to the Flory theory prediction as demonstrated in Fig. 7c.

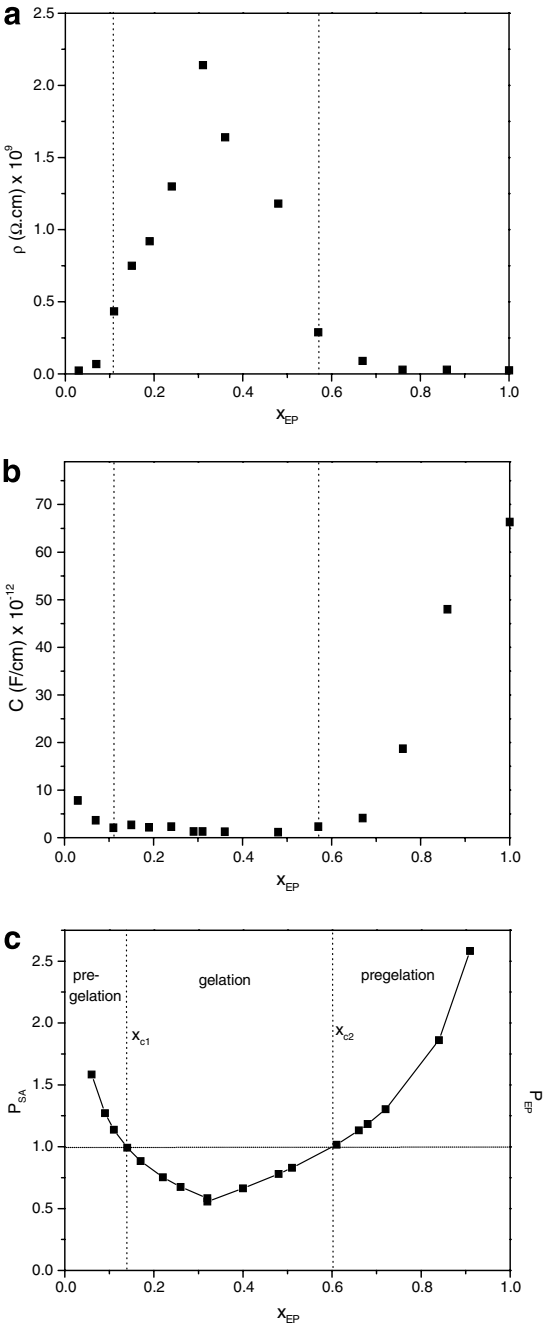

Fig. 7. (a) The relation between resistivity (ρ) and epoxy molar function (x_{EP}), (b) relation between capacitance (C) and epoxy molar function (x_{EP}) and (c) the theoretically expected behavior of P_{EP} and P_{CH} as function of x_{EP}.

Fig. 7a shows the behavior of the resistivity (ρ) obtained by using the Bode diagram as a function of the epoxy molar fraction (x_{EP}). The resistivity changes from a low value in the anhydride excess increasing to a maximum near the stoichiometric formulation ($x_{EP} = 0.31$) and then decreases again until low values in the samples with epoxy excess. The stoichiometric composition presents the highest value of resistivity. In fact, this can be related to the density of the three-dimensional net produced during the curing process. The stoichiometric sample presents a more dense spatial interconnectivity than the other samples. The spatial interconnectivity surely affects the electric properties of the material.

The evaluation of the capacitance of samples with different molar compositions is important because it is directly related to the complex dielectric constant of the material through the Debye theory. Fig. 7b shows a plot of the capacitance (C) as a function of epoxy molar fraction (x_{EP}). It can be observed that the total capacitance of the system passes through a minimum in the x_{EP} range between 0.10 and 0.57. This means that the cured system demonstrates a decreasing charge storing capability near the stoichiometric formulation, which is in accordance with the increasing resistivity behavior.

In order to elucidate the dielectric behavior of the system a discussion of the gelation according to the Flory conceptions can be helpful. According to the Flory theory [28,30,31] the conditions for the formation of an infinite network can be derived from de critical branching coefficient β_c which is related to the functionality (g) of the reactants (Eq. (22)), in this case the epoxy and the anhydride.

$$\beta_c = (g-1)^{-1}. \tag{22}$$

In general, the branching coefficient β is related to de fractions of anhydride groups and epoxy groups present in the reactional mixture which are given by $P_{EP}$and P_{SA}. As already discussed by Castiglia et al. [27] and Nucci et al. [29] considering functionality 2 for the anhydride and 4 for the epoxy, the theoretically expected behavior of P_{EP} and P_{SA} as function of x_{EP} is demonstrated in Fig. 7c. The two critical composition conditions are given by $x_{EP1} = 0.14$ and $x_{EP2} = 0.60$, respectively. In other words, theoretically, no gelation occurs in the x_{EP} regions from 0.00 to 0.14 and from 0.60 to 1.00 because the values P_{EP} and P_{SA} greater than 1 correspond to nonphysical values of the fraction of reacted anhydride and epoxy groups. Castiglia et al. [27] studying by Temperature Scanning

Brillouin Spectroscopy (TSBS) a similar epoxy system obtained experimentally the pregelation regions x_{EP}: 0.00 − 0.14 (SA excess) and x_{EP}: 0.56–1.00 (EP excess), that are in good agreement with the theoretical values x_{EP1} and x_{EP2}.

Fig. 7a–c shows in a comparative way, the behavior of the resistivity, the capacitance and the theoretically calculated parameters P_{SA} and P_{EP} as functions of x_{EP}. Both experimentally obtained properties, resistivity and capacitance, present strong changes near the x_{c1} and x_{c2} predicted by using Flory theory. The resistivity, practically, remains constant for x_{EP} values smaller than 0.10 and greater than 0.57. The values lie very near to the theoretical values $x_{c1} = 0.14$ and $x_{c2} = 0.60$. The capacitance behaves the same way, but in the inverse mode, as expected. It is to conclude that the EIS demonstrates sensitivity and is capable to detect physical phase changes.

4.3. Relaxation processes

In order to evaluate the relaxation dielectric processes of the studied epoxy system, complex electric properties: $\varepsilon^\bullet$, $Y^\bullet$, $M^\bullet$, $Z^\bullet$, and $\tan\delta$ were used as frequency depended functions. According to Gerhardt et al. [32,33] every one of these functions presents a distinct relaxation time; however they are related each other. Generally, every relaxation process has one relaxation time which value depends on the choice of the representing electric function. Relations between various relaxation times have been established for three basic models: (a) Debye, (b) Cole–Cole and (c) ideal conduction. In all three cases, the relaxation times, if they exist, are related by

$$\tau_\varepsilon \tau_M = \tau_Z \tau_Y = \tau^2_{\tan\delta} \tag{23}$$

or

$$(\log\tau_\varepsilon + \log\tau_M)/2 = (\log\tau_Z + \log\tau_Y)/2 = \log\tau_{\tan\delta}. \tag{24}$$

This means that, on logarithmic scale, the average relaxation time for any pair of inverse complex function ($\varepsilon^\bullet M^\bullet = Z^\bullet Y^\bullet = 1$) is equal to the loss tangent relaxation time and not related to any other parameters. In addition, they follow the order:

$$\tau_\varepsilon \geqslant \tau_Y > \tau_{\tan\delta} > \tau_Z \geqslant \tau_M. \tag{25}$$

Considering the same relaxation process for all five possible electric functions, it is to expect [32,33] that the imaginary part of the dielectric constant (ε'') demonstrates the relaxation in the lowest frequency while the electric modulus imaginary part (M'') would be find in the relatively highest frequencies. The values of the relaxation times and the difference between them depend on the relaxation ratio $r = \varepsilon_r/\varepsilon_u$. The obtained relations are important for the correct frequency data analysis and can be used to calculate one relaxation time for another. According to these relations, a relaxation peak characteristic of one electric function may be seen or not seen at all, within a limited frequency range available experimentally [32,33]. However, there is always a frequency range where the relaxation peak may be found.

In this study, from the five used electric functions, only the M'', Z'' and $\tan\delta$ indicate presence of relaxation peak when analyzed as frequency functions. Fig. 8a–c shows representative relaxation curves of M'', Z'' and $\tan\delta$ for samples with the same composition ($X_{EP} = 0.07$).

4.3.1. The M'' relaxation

Fig. 8a show a representative diagram of M'' versus $\log f$ obtained for the $x_{EP} = 0.07$ sample. Using the frequencies f_p where Z'' reaches the maximum we calculated the corresponding time constants or relaxation time according to Eq. (26):

$$\tau = \frac{1}{2\pi f_p}. \tag{26}$$

In Table 3 the obtained $\tau_{M''}$ values for all studied compositions are presented. According to this table, a shift of the $\tau_{M''}$ from lower to higher values is observed when the system moves from the high anhydride and epoxy excess to the stoichiometric composition.

4.3.2. The Z'' relaxation

Fig. 8b presents the relaxation curve Z'' versus $\log f$ obtained for the formulation $x_{EP} = 0.07$. All studied formulations present similar relaxation curves in the experimental frequency range. Similar to the frequency behavior of M'', it was observed that the frequency position of the maximum Z'' relaxation curve shifts to lower frequencies and the corresponding time constant increases when the chemical composition of the epoxy system approximates the stoichiometric one, as given in Table 3.

4.3.3. The $\tan\delta$ relaxation

In the representation of the $\tan\delta \times \log f$ it was observed that only the samples with compositions

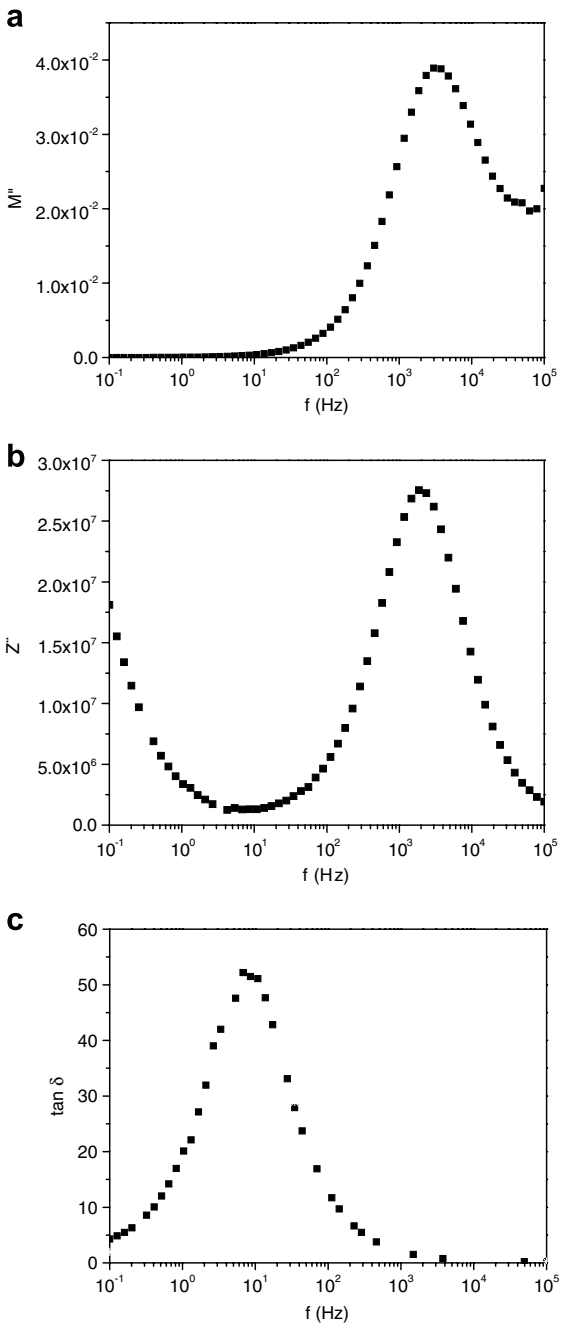

Fig. 8. (a) M'' versus $\log f$; (b) Z'' versus $\log f$ and (c) $\tan\delta$ versus $\log f$ for $x_{EP} = 0.07$.

of $x_{EP} = 0.03$ and $x_{EP} = 0.07$ (Fig. 8c) presented relaxation peak. The variation of the composition shits the relaxation peaks out of the experimentally available frequency range.

The values of $\tau_{M''}, \tau_{Z''}$ and $\tau_{\tan\delta}$ confirm the theoretically expected behavior predicted by Gerhardt [32,33] where for the same relaxation process, $\tau_{\tan\delta}$ must be greater than $\tau_{Z''}$ and this greater than $\tau_{M''}$.The relaxation peaks of tanδ would appear in lower frequencies as expected for charge migration processes [3–10]. The obtained relaxation results for M'', Z'' and $\tan\delta$ permit to affirm that probably the same relaxation process is responsible for the electric behavior of the studied epoxy system. It is expected that the observed relaxation process is related to the charge migration inside the macro and supra-molecular structure of the epoxy material.

Table 3
$\tau_{M''}, \tau_{Z''}$ and $\tau_{(\tan\delta)}$ associated to different epoxy molar fraction compositions

x_{EP}	$\tau_{M''}$ (μs)	$\tau_{Z''}$ (μs)	$\tau_{\tan\delta}$ (μs)
0.03	68	33	19000
0.07	135	85	7300
0.10	650	502	–
0.14	970	1120	–
0.18	1710	1410	–
0.24	2800	1780	–
0.31	3100	1780	–
0.36	2370	1410	–
0.48	2200	1120	–
0.57	590	400	–
0.67	140	217	–
0.76	140	217	–
0.86	140	217	–
1.00	35	170	–

5. Conclusions

Electric impedance spectroscopy was performed in epoxy system (EP/succinic anhydride/TEA) over a wide range of compositions, including mixtures with anhydride excess, stoichiometric for-mulation, epoxy excess and constant TEA molar fraction.

The aspects related to: (a) the resistivity and capacitance and (b) the relaxation process of the different electric functions (ε^*, M^*, Z^*, Y^* and $\tan\delta$) of the samples with different compositions have been discussed the first in relation to the Flory theory and the second according to the Gerhardt prediction of the relaxation times obtained by different electric functions.

The sample resistivity was obtained in the low frequency regime where the polarization due to migrating charges dominates the electric response of the polymer. The resistivity (ρ) starts increasing abruptly with $x_{EP} = 0.10$, reaches a maximum in the stoichiometric sample, decreases strongly until $x_{EP} = 0.57$ and then remains practically constant. The capacitance as a function of molar fraction composition x_{EP} presents minimum values in the

range between x_{EP} 0.10 and 0.57. The x_{EP} values 0.10 and 0.57 are very near to the gelation critical concentrations $x_{c1} = 0.14$ for the anhydride excess and $x_{c2} = 0.60$ for the epoxy excess as predicted by Flory theory. In the studied system, the Electric Impedance Spectroscopy is capable to detect the change from the pre-gel to gel phase.

Relaxation peaks have been detected in the M'' and Z'' frequency dispersion analysis for all studied samples with x_{EP} from 0.03 up to 1.0 in the frequency range 10^{-1} to 10^{5} Hz. However, the $\tan\delta$ frequency analysis, presents relaxation peaks only for the samples with composition $x_{EP} = 0.03$ and $x_{EP} = 0.07$. The relaxation times $\tau_{M''}$, $\tau_{Z''}$ and $\tau_{\tan\delta}$ indicate that the relaxation process is related to the charge migration process. The relaxation results obtained by using the Z'', M'' and $\tan\delta$ formalism are in accordance with the theoretical prediction of Gerhardt. The results of this study demonstrated the applicability of the Gerhand prediction to other systems, in this case epoxy with different compositions, additionally to the metal oxides and silica coated with alkali previously studied.

References

[1] Adams LV, Gannon JA. Epoxy resins: Encyclopedia of polymer science and engineering. New York: John Wiley and Sons; 1996.
[2] May CA. Epoxy resins chemistry and technology. New York: Marcel Dekker, Inc.; 1988.
[3] Bellucci F, Valentino M, Monetto T, Nicodemo L, Kenny J, Nicolais L, et al. J Polym Sci Part B: Polym Phys 1994; 32:2519.
[4] Mijovic J, Bellucci F, Nicolais L. J Electrochem Soc 1995;142:1176.
[5] Bellucci F, Valentino M, Monetto T, Nicodemo L, Kenny J, Nicolais L, et al. J Polym Sci Part B: Polym Physics 1995; 33:433.
[6] Mijovic J, Andjelic S, Fitz B, Zurowsky W, Mondragon I, Belluccio F, et al. J Polym Sci Part B: Polym Phys 1996; 34:379.
[7] Mijovic J, Kenny JM, Maffezzoli A, Trivisano A, Bellucci F, Nicolais L. Compos Sci Technol 1993;49:277.
[8] Mijovic J, Andjelic S, Winnie Yee CF. Macromolecules 1995;28:2797.
[9] Mijovic J, Winnie Yee CF. Macromolecules 1994;27:7287.
[10] Kranbuehl DE, Delos SE, Jue PK. Polymer 1986;27:11.
[11] Zukas WX. Macromolecules 1993;26:2390.
[12] Eloundou JP. Eur Polym J 2002;38:431.
[13] Psarras GC, Manolakaki E, Tsangaris GM. Compos: Part A 2002;33:375.
[14] Gallone G, Levita J, Mijovic S, Andjelic S, Rolla P. Polymer 1998;39:2095.
[15] Fitz DB, Mijovic J. Macromolecules 1999;32:4134.
[16] Mijovic J. J Non Cryst Solids 1998;235–237:587.
[17] Fitz B, Andjelic S, Mijovic J. Macromolecules 1997;30:5227.
[18] Andjelic S, Fitz B, Mijovic J. Macromolecules 1997;30:5239.
[19] Pethrick R, Hayward D. Progr Polym Sci 2002;27:1983.
[20] Montsserat S, Roman F, Colomer P. Polymer 2002;44:101.
[21] Kremer F. J Non Cryst Solids 2002;305:1.
[22] Corezzi S, Capaccioli S, Gallone G, Lucchesi M, Rolla PA. J Phys Condens Matter 1999;11:10297.
[23] Levita G, Livi A, Rolla PA, Culicchi C. J Polym Sci Part B: Polym Phys 1996;34:2731.
[24] Nixdorf K, Busse G. Compos Sci Technol 2001;61:889.
[25] Samios D, Castiglia S, Silveira NP, Stassen H. J Polym Sci Part B: Polym Phys 1995;33:1857.
[26] Miranda MI, Tomedi C, Bica CID, Samios D. Polymer 1997;38:1017.
[27] Miranda MI, Bica CID, Samios D. Polymer 1997;38:4843.
[28] Castiglia S, Fioretto D, Verdini L, Samios D. J Polym Sci Part B: Polym Phys 2001;39:1326.
[29] Nucci AM, Nicolau A, Martini EMA, Samios D. Eur Polym J 2006;42:195.
[30] Flory PJ. Principles of Polymer Chemistry. New York: Cornell University Press; 1953.
[31] Apicella A, Beretta CA, Castiglione-Morelli MA, Martuscelli E, Nicolais L, Nobile MR. J Therm Anal 1985;30:1349.
[32] Cao W, Gerhardt R. Solid State Ionics 1990;42:213.
[33] Gerhardt R. J Phys Chem Solids 1994;55:1491.